

Normal pregnancy induced glucose metabolic stress in a longitudinal cohort of healthy women

Novel insights generated from a urine metabolomics study

Mu Wang, PhD^{a,b}, Wei Xia, PhD^b, Han Li, PhD^b, Fang Liu, PhD^a, Yuanyuan Li, PhD^b, Xiaojie Sun, PhD^b, Songfeng Lu, PhD^{a,*}, Shunqing Xu, PhD^{b,*}

Abstract

During normal pregnancy, mothers face a unique physiological challenge in the adaptation of glucose metabolism in preparation for the metabolic stress presented by fetal development. However, the responsible mechanism remains elusive. The purpose of this study is to investigate the mechanism of the metabolic stress of glucose metabolism in pregnant women using metabolomics method.

A Ultra Performance Liquid Chromatography Quadrupole Time-of-Flight Mass Spectrometer-based untargeted metabolomics study was performed to investigate the dynamic urinary signature of the intermediates of glucose metabolism in a longitudinal cohort of 232 healthy pregnant women in their first, second, and third trimesters.

Twelve glucose metabolic intermediates were screened out from hundreds of candidate metabolites using partial least squares discriminant analysis models. These 12 markers were mainly involved in the metabolic pathways of insulin resistance, glycolysis/gluconeogenesis, tricarboxylic acid cycle, nonabsorbable carbohydrate metabolism, and N-glycan biosynthesis. In particular, L-acetylcarnitine, a metabolite that is beneficial for the amelioration of insulin resistance, decreased in a time-dependent manner during normal pregnancy. Moreover, thiamine pyrophosphate, an intermediate product of glycolysis/gluconeogenesis, significantly increased in the second trimester, and argininosuccinic acid and oxalosuccinic acid, intermediates involved in the tricarboxylic acid cycle, significantly decreased in the third trimester, suggesting an increased glucose demand in the maternal body during fetal development.

These findings provide novel insight into the normal pregnancy-induced elevation of insulin resistance and glycolysis/gluconeogenesis, as well as the observed reduction in the aerobic oxidation of glucose.

Abbreviations: ESI = electrospray ionization, FC = fold change, GCDC = glycochenodeoxycholic acid, GDM = gestational diabetes mellitus, GWAS = genome-wide association studies, KEGG = Kyoto Encyclopedia of Genes and Genomes, PCA = principal component analysis, PLS-DA = partial least squares discriminant analysis, QC = quality control, RT = retention time, SDSD = standard deviation step down, UPLC-MS = Ultra Performance Liquid Chromatography Mass Spectrometer, UPLC-QTOFMS = Ultra Performance Liquid Chromatography Quadrupole Time-of-Flight Mass Spectrometer, VIP = variable importance in projection.

Keywords: glucose metabolism, metabolomics, normal pregnancy, pregnancy cohort

1. Introduction

During pregnancy, mothers face a unique physiological challenge that requires complex adaptation coordinated by placenta- and nonplacenta-derived hormones to prepare for the metabolic stress presented by fetal development and to ensure the accurate

and adequate shunting of nutrients from themselves to the fetus.^[1–3] Of particular importance during pregnancy is the maintenance of glucose homeostasis.^[3] Glucose metabolism during normal pregnancy is characterized by an impairment in insulin sensitivity, an increase in β -cell secretory response and

Editor: Gaurav Malhotra.

This work was supported by the National Natural Science Foundation of China (21437002, 81372959, 81402649, and 21407117), the R&D Special Fund for Public Welfare Industry (Environment) (201309048), and the National Basic Research Program of China (973 Program) (2012CB722401). This work was also supported by the Natural Science Foundation of Hubei Province (2016CFB541) and the Applied Basic Research Program of Wuhan Science and Technology Bureau (20160101010003).

The authors have no conflicts of interest to disclose.

Supplemental Digital Content is available for this article.

^a School of Computer Science and Technology, Huazhong University of Science and Technology, ^b Key Laboratory of Environment and Health, Ministry of Education and Ministry of Environmental Protection, and State Key Laboratory of Environmental Health (Incubation), School of Public Health, Tongji Medical College, Wuhan, Hubei, China.

* Correspondence: Shunqing Xu, Key Laboratory of Environment and Health, Ministry of Education and Ministry of Environmental Protection, and State Key Laboratory of Environmental Health (Incubation), School of Public Health, Tongji Medical College, Huazhong University of Science and Technology, Wuhan, Hubei, China (e-mail: xust@hust.edu.cn); Songfeng Lu, School of Computer Science and Technology, Huazhong University of Science and Technology, Wuhan, Hubei, China (e-mail: lusongfeng@hotmail.com).

Copyright © 2018 the Author(s). Published by Wolters Kluwer Health, Inc.

This is an open access article distributed under the terms of the Creative Commons Attribution-Non Commercial-No Derivatives License 4.0 (CCBY-NC-ND), where it is permissible to download and share the work provided it is properly cited. The work cannot be changed in any way or used commercially without permission from the journal.

Medicine (2018) 97:40(e12417)

Received: 22 December 2017 / Accepted: 19 August 2018

<http://dx.doi.org/10.1097/MD.00000000000012417>

β -cell mass, a moderate increase in blood glucose levels following the ingestion of a meal, and changes in the levels of circulating free fatty acids, triglycerides, cholesterol, and phospholipids.^[1,2] These changes seem to be a necessary and indispensable physiological response to meet the energy demand of fetal development and to provide additional energy storage for labor and lactation.^[1] However, the mechanisms underlying the adaptive changes in glucose metabolism are not well understood.

“Omic” technologies have been recently recognized as a promising approach that is capable of providing novel insight into the pathogenic mechanisms of maternal-fetal medicine.^[3–10]

In genome-wide association studies (GWAS), the adaptations in glucose metabolism associated with the physiological changes in insulin sensitivity and β -cell functional traits that occur during normal pregnancy overlap with those observed in nonpregnant populations and in individuals with type 2 diabetes.^[3,11–15] Genetic loci such as *CDK5 Regulatory Subunit Associated Protein 1-like 1 (CDKAL1)*, *Glucokinase (GCK)*, *Glucokinase Regulator (GCKR)*, *Hexokinase Domain Containing 1 (HKDC1)*, and *Beta-site APP-Cleaving Enzyme 2 (BACE2)* were found to be associated with glycemic traits identified in studies using cohorts of pregnant subjects.^[3,11–15] However, the genotypic associations between pregnancy and diabetes are insufficient to reveal the exact mechanisms underlying the phenotype of glucose metabolic stress during healthy gestation. Metabolomics studies, which strongly complement GWAS, provide a qualitative and quantitative description of the low molecular mass endogenous metabolites present in a biological sample such as urine, plasma, or tissue.^[16] In addition, metabolomics studies have confirmed that the higher circulating concentrations of key metabolites, including branched-chain amino acids and their metabolites, in patients with type 2 diabetes and gestational diabetes mellitus (GDM) are associated with insulin sensitivity, pancreatic β -cell function, and insulin resistance.^[17–19] Although these metabolomics studies contribute considerably to the understanding of pregnancy complications associated with glucose metabolism, they allow limited conclusions about the physiological adaptation of glucose metabolic stress during normal pregnancy among healthy women.

Driven by previous GWAS results that indicate similarities in glucose metabolism during normal, healthy pregnancy and in diabetes and by the relative information gap regarding the responsible mechanisms, we conducted an Ultra Performance Liquid Chromatography Quadrupole Time-of-Flight Mass Spectrometer (UPLC-QTOFMS)-based untargeted urine metabolomics analysis in a longitudinal cohort of 232 healthy pregnant women to investigate dynamic variations in glucose metabolism-associated metabolite profiles and metabolic pathways during the course of normal pregnancy. A partial least squares discriminant analysis (PLS-DA) combined with a standard deviation step down (SDSD) method allowed more focus on metabolite concentration than is possible with false discovery rate (FDR) methods, reduced type II error rates and improved statistical efficiency.^[20]

2. Methods

The participants in this study were selected from the healthy pregnant women who were treated at the Maternal and Child Health Hospital of Wuhan City in China between November 2013 and July 2014 ($n=286$). In the present study, we excluded participants who were lost to follow-up during the whole course of pregnancy ($n=48$) and those with multiple pregnancies ($n=4$), as well as those who suffered GDM ($n=2$). A total of 232 subjects

were eventually considered valid for the present study. All participants provided written informed consent and completed an individual questionnaire at the time of urine sample collection for this study. Each subject was followed up until delivery to ensure that the women had normal-term pregnancies and healthy babies. Clinical information was obtained from face-to-face interviews and obstetrical and neonatal medical records. Subjects, who were more than 18 years old; had a singleton, intrauterine pregnancy, and were nondiabetic, were eligible for inclusion in the present cohort study. A total of 696 urine samples from 232 healthy subjects were collected at 3 different time points: the first trimester, the second trimester, and the third trimester. Detailed information about the demographic characteristics of these subjects is shown in Supplementary Table S1, <http://links.lww.com/MD/C515>. The urine samples were frozen at -80°C until analysis. The number of freeze–thaw cycles was minimized to reduce the introduced interference as much as possible. To minimize the possible interference of system error in the analysis, the UPLC-QTOFMS tests were randomized by dividing all the testing samples into 3 homogeneous blocks (T1, T2, and T3), each of which had an equal sample size. The research protocol was approved by the Ethics Committees of the Tongji Medical College, the Huazhong University of Science and Technology, and the study hospital. All experiments were performed in accordance with the principles expressed in the Declaration of Helsinki or other relevant guidelines and regulations.

2.1. High throughput metabolic profiling spectral acquisition

2.1.1. Ultra performance liquid chromatography. Chromatographic analysis was performed with an Acquity Ultra Performance liquid chromatography system (Waters Technologies [Shanghai] Ltd., China) with an ACQUITY UPLC HSS T3 column (2.1×100 mm, $1.8 \mu\text{m}$, Waters). Mobile phase A was 0.1% formic acid in water (v/v) and mobile phase B was 0.1% formic acid in methanol (v/v); the flow rate was 0.5 mL/min. The gradient conditions of the mobile phase in positive and negative mode were as follows: 0 to 1 minute: 1% B; 1 to 3 minutes: 1% to 15% B; 3 to 6 minutes: 15% to 50% B; 6 to 9 minutes: 50% to 95% B; 9 to 10 minutes: 95% B; 10 to 10.1 minutes: 95% to 1% B; and 10.1 to 12 minutes: 1% B. The temperature of the column and the autosampler was maintained at 40 and 4°C , respectively.^[21]

2.1.2. Mass spectrometry. A Waters Synapt High-Definition Time-of-Flight Mass Spectrometry system (Waters) equipped with an electrospray ionization (ESI) source operating in positive and negative mode was connected to the UPLC system and used in this study. The capillary voltage was 3.2 and 2.4 kV in the positive and negative ionization modes, respectively. The desolvation temperature was 350°C , the sampling cone voltage was 40 V, the extraction cone voltage was 4.0 V, the source temperature was 120°C , the cone gas flow was 2.5 L/h, and the desolvation gas flow was 900 L/h. To ensure accurate mass measurement, the mass was corrected with leucine-enkephalin during acquisition to generate a reference ion at m/z 556.2771 Da ($[\text{M} + \text{H}]^{+}$) in positive ion mode and m/z 554.2615 Da ($[\text{M} - \text{H}]^{-}$) in negative ion mode before the instrument was used.

2.1.3. Quality control, data analysis, and metabolite identification. The quality control (QC) method was applied to evaluate the repeatability of the metabolomics method. An equal volume of $10 \mu\text{L}$ of each tested urine sample was mixed thoroughly to prepare the pooled QC samples. At the beginning and the end of

each batch of Ultra Performance Liquid Chromatography Mass Spectrometer (UPLC-MS) analysis, 5 QC samples were injected, and then 1 QC sample was tested at a regular interval of every 10 samples.^[21] If the coefficient of variation was more than 20%, the variables were deleted. The acquired UPLC-MS data were analyzed in MassLynx V4.1 software (Waters). The 3-dimensional matrix of the ion intensities, retention time (RT), and *m/z* value was constructed for each metabolite feature.

The unsupervised data analysis method of principal component analysis (PCA) was performed on all the samples to evaluate the robustness of the metabolic profiling platform. PLS-DA was used to analyze the difference between the sample groups. In this study, unit variance scaling was applied to avoid the mask effect. Variables with a variable importance in projection (VIP) value >1 were screened out for further statistical testing.

A decision tree algorithm was used to select the statistical significance test for the variables screened out by PLS-DA.^[22] Compared with FDR methods, the SDS method allowed more focus on information about the metabolite concentration. This method was introduced in this study to reduce the rate of type II errors and to improve the statistical efficiency.^[20] Variables that passed the SDS test and had a VIP > 1 were considered potential markers in the next step of metabolite identification.

Several ion adducts, including $[M - H]^-$, $[M + HCOO]^-$, $[2M - H]^-$, $[M + H]^+$, $[M + NH_4]^+$, $[M + Na]^+$, $[M + K]^+$, $[2M + H]^+$, $[2M + H + K]^{2+}$, and $[2M + H + Na]^{2+}$, were present in both positive and negative mode high-resolution ESI. These adducts make the identification of metabolites difficult because the accurate calculation and comparison of each type of adduct is very time-consuming. To rapidly identify a metabolite, we used software that was developed for batch processing of automatic putative identification by matching the measured *m/z* data list with a reference *m/z* data list derived from the HMDB database.^[23] The key metabolites were further confirmed by the comparison of their fragmentation patterns and structural information with those obtained from the HMDB, METLIN, or MassBank databases.

2.1.4. Data visualization and biomarker network analysis.

The relative concentration of glucose metabolic intermediates in the corresponding trimesters of pregnancy for each subject was further scaled to a value between 0 and 1 by a “for” loop statement in R (R Core Team (2015). R: A language and environment for statistical computing. R Foundation for Statistical Computing, Vienna, Austria: <https://www.R-project.org/>). Heat maps with a clustering tree were also created in R. Detailed chemical and biological information about the significant metabolites from the comparison between the different trimesters of pregnancy was retrieved online at “<https://pubchem.ncbi.nlm.nih.gov/>” and “<http://www.kegg.jp/>.” The network software MetaMapp (<http://metamapp.fiehnlab.ucdavis.edu/homePage>) was used to generate node and edge data for the metabolite network with the Cytoscape software.^[24]

3. Results

By using the UPLC-QTOFMS analysis protocol and subsequent processes, more than 3000 exact mass RT pairs were detected in the positive ion mode and negative ion mode. The PCA results showed that the QC samples were well clustered in the score plots (Supplementary Fig. S1, <http://links.lww.com/MD/C515>), indicating the absence of obvious drifts in the UPLC-QTOFMS platform in the present study. Moreover, as shown in the PLS-DA

score plots (Figs. 1A, B and 2A, B), there were obvious distinctions between the second trimester (T2) and the first trimester (T1), as well as between the third trimester (T3) and the second trimester (T2), in both ion modes. The fit of the PLS-DA model was assessed by the values of R^2Y and Q^2 in the cross-validation, with the former term indicating the goodness of fit and the latter indicating the goodness of prediction. In the positive ion mode, the cross-validation values of R^2Y and Q^2 were 0.901 and 0.861, respectively, in the comparison between T2 and T1 and were 0.918 and 0.867, respectively, in the comparison between T3 and T2. In the negative ion mode, the cross-validation values of R^2Y and Q^2 were 0.851 and 0.813, respectively, in the comparison between T2 and T1 and were 0.652 and 0.607, respectively, in the comparison between T3 and T2. To further validate whether the PLS-DA models were overfitted, 999 permutation tests were performed in the present study. As shown in the permutation test plots (Figs. 1C, D and 2C, D), the intercepts for the PLS-DA models did not achieve the threshold for overfitting ($R^2Y > 0.4$, $Q^2Y > 0.05$), indicating that the PLS-DA models in this study were established effectively.

When the condition of VIP > 1 was applied, 667 metabolites were putatively identified in the positive ion mode, and 425 metabolites were putatively identified in the negative ion mode. These metabolites were mainly involved in the metabolism of glucose, amino acids, and nucleosides. Supplementary Tables S2, <http://links.lww.com/MD/C515>, and S3, <http://links.lww.com/MD/C515>, show the top 50 metabolites in positive ion mode and negative ion mode ranked by VIP value. After SDS correction, Kyoto Encyclopedia of Genes and Genomes (KEGG) pathway analysis, and mass spectrum/mass spectrum (MS/MS) fragment pattern validation, we found that 8 glucose metabolic intermediates significantly changed between the second trimester (T2) and the first trimester (T1) and that 8 glucose metabolic intermediates significantly changed between the third trimester (T3) and T2 (Tables 1 and 2). Supplementary Table S4, <http://links.lww.com/MD/C515>, shows the normal pregnancy-related markers involved in glucose metabolism that were identified in the urine of healthy pregnant women.

3.1. Maternal urinary metabolites involved in glucose metabolism

The dynamic change in and the intersection at different time points for these glucose metabolic intermediates are shown in Fig. 3. As shown in Fig. 3A, 4 overlapping metabolites and 4 exclusive metabolites were screened out for T2 versus T1 and T3 versus T2, respectively. In this study, L-acetylcarnitine showed a time-dependent decrease, while glycochenodeoxycholic acid (GCDC) 3-glucuronide showed a time-dependent increase, during the course of pregnancy; 2-phenylethanol glucuronide was significantly increased in T2 but was decreased in T3; 6-dehydrotestosterone glucuronide was significantly decreased in T2 but was increased in T3; 3 metabolites (1,4-beta-D-glucan, D-glucuronic acid 1-phosphate, and dolichol phosphate) were decreased significantly in T2 and were maintained at a low level in T3; 3 metabolites (galactosylglycerol, argininosuccinic acid, and oxalosuccinic acid) did not show a remarkable change in T2 but were significantly decreased in T3; 2-keto-glutaramic acid did not show a remarkable change in T2 but was significantly increased in T3; and thiamine pyrophosphate increased significantly in T2 and was maintained at a high level in T3 (Fig. 3B).

The relative concentrations of the metabolites that were significantly changed in each subject were further visualized with

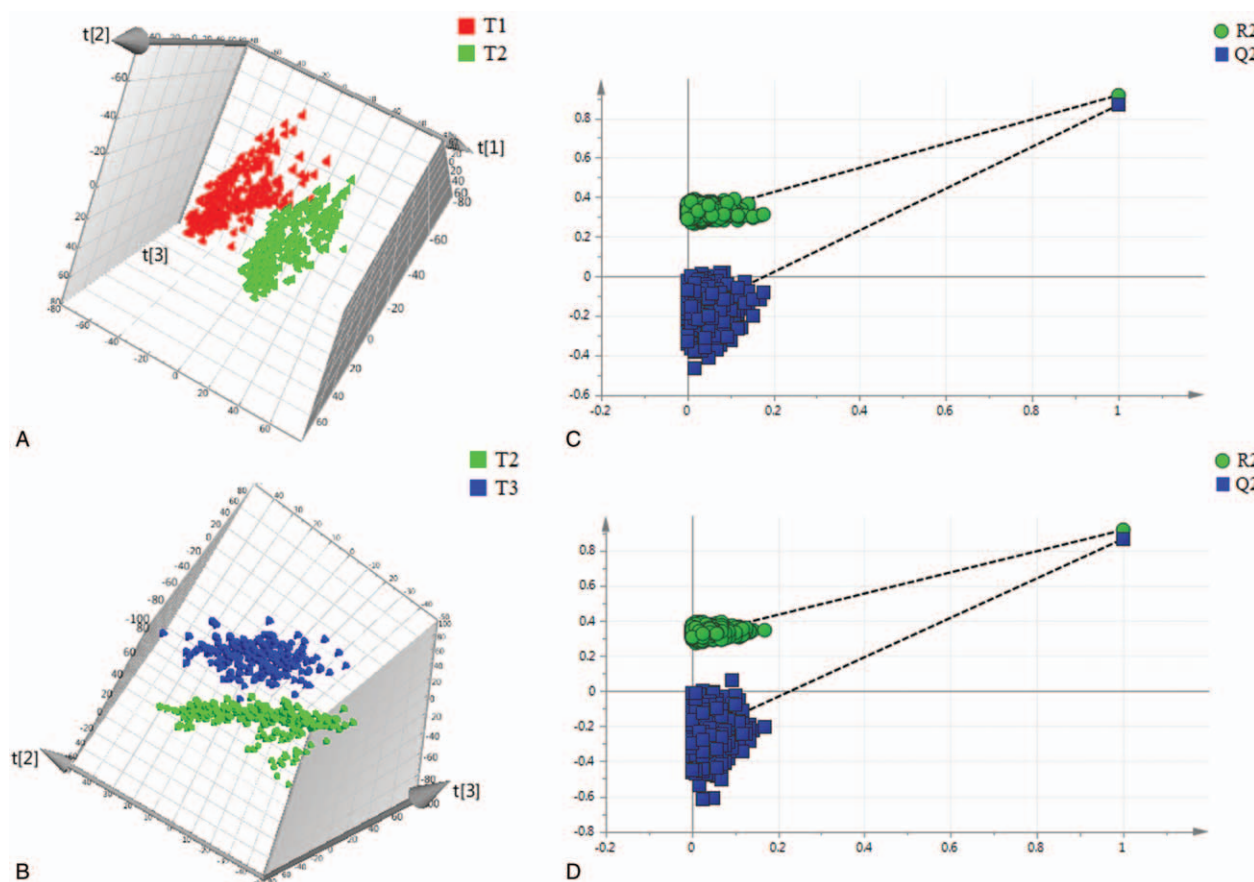


Figure 1. Differentiation of urine metabolic profiles from healthy pregnant women obtained in positive ion mode using PLS-DA models. (A) PLS-DA analysis between the first trimester and the second trimester. (B) PLS-DA analysis between the second trimester and the third trimester. (C) 999 permutation test for the PLS-DA model of the comparison between the first trimester and the second trimester. (D) 999 permutation test for the PLS-DA model of the comparison between the second trimester and the third trimester. $t[1]$, $t[2]$, and $t[3]$ denote the first component, the second component, and the third component, respectively. T1, T2, and T3 denote the first trimester, the second trimester, and the third trimester, respectively. PLS-DA = partial least squares discriminant analysis.

a heat map (Fig. 4). The metabolite concentrations were visualized with a red-to-green color gradient. Red represented low-abundance metabolites, green represented high-abundance metabolites and black represented moderate-abundance metabolites. From the heat map, the changing trends in the corresponding metabolites in the different groups could be easily observed simultaneously.

3.2. Network reconstruction for normal pregnancy-induced glucose metabolic changes

“Biochemistry” refers to the conversion of chemically similar compounds by catalytic enzymes, which makes it seem logical to associate all compounds directly by their chemical similarity; thus, clusters of chemically similar compounds should then resemble biochemical modules.^[25] Under this background, we calculated the chemical similarity matrix for the studied metabolites using the PubChem database and found that the metabolites that had high similarity were most likely derived from the same biochemical pathway.^[25]

In addition to the chemical similarity information, we also retrieved the biochemical information about the studied metabolites from the KEGG pathway database. Of the 4 overlapping metabolites, L-acetylcarnitine was involved in insulin resistance (KEGG map ID: map04931), and the other 3

metabolites (2-phenylethanol glucuronide, 6-dehydrotestosterone glucuronide, and GCDC 3-glucuronide) were involved in pentose and glucuronate interconversions (KEGG map ID: map00040). Of the 4 exclusive metabolites in the T2 versus T1 comparison, 1,4-beta-D-glucan was involved in carbohydrate digestion and absorption (KEGG map ID: map04973), thiamine pyrophosphate was involved in glycolysis/gluconeogenesis (KEGG map ID: map00010), D-glucuronic acid 1-phosphate was involved in pentose and glucuronate interconversions (KEGG map ID: map00040), and dolichol phosphate was involved in N-glycan synthesis (KEGG map ID: map00510). Of the 4 exclusive metabolites in the T3 versus T2 comparison, galactosylglycerol was involved in galactose metabolism (KEGG map ID: map00052), argininosuccinic acid and oxalosuccinic acid were involved in the citrate cycle (tricarboxylic acid cycle [TCA cycle], KEGG map ID: map00020), and 2-keto-glutaramic acid was involved in glycogenic amino acid metabolism (KEGG map ID: map00250).

In this study, to better visualize the differences in metabolic regulation induced by normal pregnancy, we applied a biochemical visualization approach using MetaMapp and Cytoscape to present metabolic network graphs that included all the known biochemical reactions and the chemical structure information.^[25,26] In Figs. 5 and 6, the intermediates of glucose metabolism are denoted by colored nodes (the red nodes

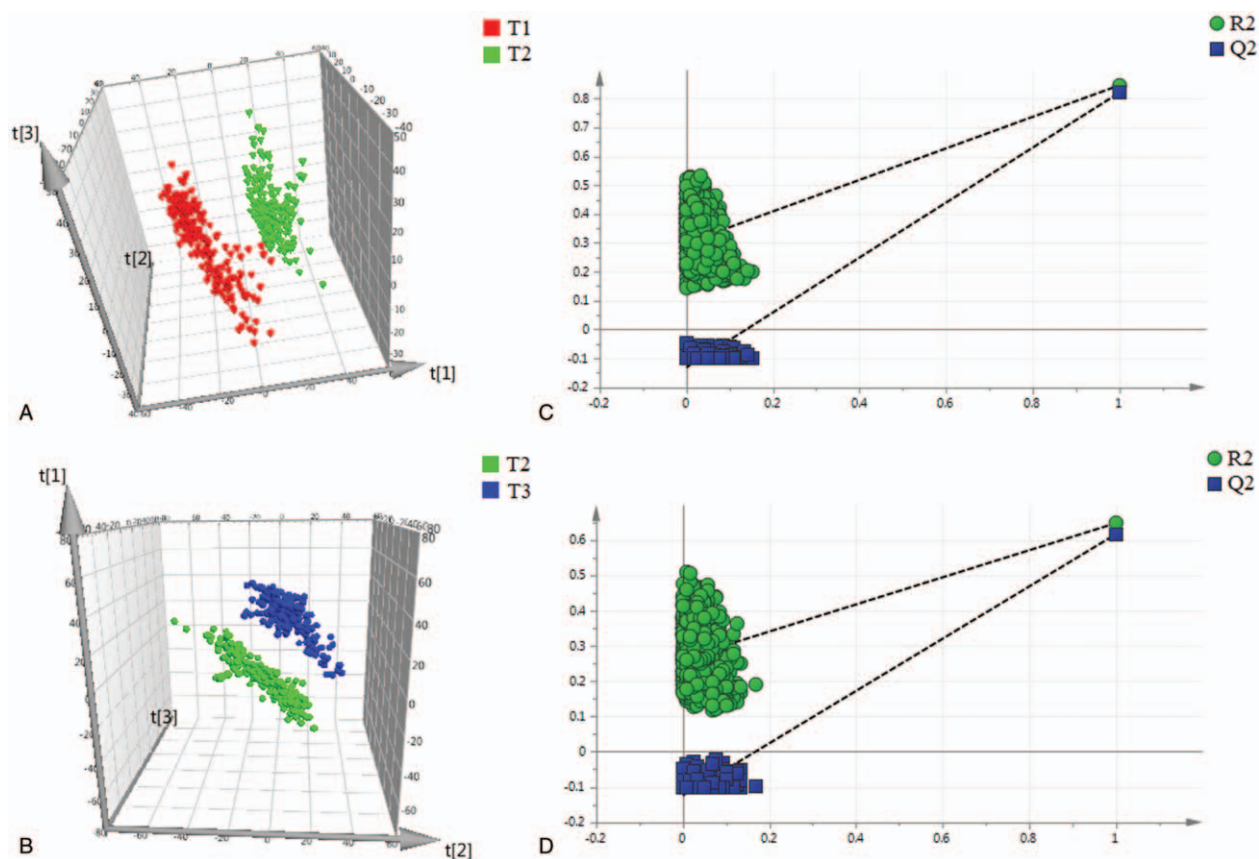


Figure 2. Differentiation of urine metabolic profiles from healthy pregnant women obtained in negative ion mode using PLS-DA models. (A) PLS-DA analysis between the first trimester and the second trimester. (B) PLS-DA analysis between the second trimester and the third trimester. (C) 999 permutation test for the PLS-DA model of the comparison between the first trimester and the second trimester. (D) 999 permutation test for the PLS-DA model of the comparison between the second trimester and the third trimester. $t[1]$, $t[2]$, and $t[3]$ denote the first component, the second component, and the third component, respectively. T1, T2, and T3 denote the first trimester, the second trimester, and the third trimester, respectively. PLS-DA = partial least squares discriminant analysis.

represent the increased metabolites, while the green nodes represent the decreased metabolites), and the node size represents the degree of change of the corresponding metabolite. The nodes representing the metabolites that were significantly changed but not involved in glucose metabolism during normal pregnancy are shown in gray, making up the overall background of the metabolic maps. As shown in the metabolic network maps (Figs. 5 and 6), the intermediates of glucose metabolism clustered into different biochemical modules, and there was a significant difference in the clustering between T2 and T1 and between T3

and T2, which both demonstrated that the features of glucose metabolic regulation changed significantly during normal pregnancy and provided novel clues in the investigation of the mechanism of pregnancy-related glucose metabolic stress.

4. Discussion

To ensure a continuous supply of nutrients and substrates for fetal development as well as additional energy stores for labor and lactation, the maternal body experiences obvious metabolic

Table 1

Significantly changed metabolites involved in glucose metabolism (T2 vs T1).

Primary ID	Retention time, min	Mass	HMDB ID	Metabolite name	P^*	FC [†]	VIP
3.89_242.0808	3.89	242.0808	HMDB00201	L-acetylcarnitine	$<5.16 \times 10^{-6}$	0.51	2.7
6.02_299.1155	6.02	299.1155	HMDB10350	2-Phenylethanol glucuronide	$<3.40 \times 10^{-6}$	3.74	2.3
6.11_571.1227	6.11	571.1227	HMDB06944	1,4-beta-D-glucan	$<1.48 \times 10^{-5}$	0.10	2.3
8.91_485.2165	8.91	485.2165	HMDB10337	6-Dehydrotestosterone glucuronide	$<9.34 \times 10^{-6}$	0.35	2.2
3.03_445.0331	3.03	445.0331	HMDB01372	Thiamine pyrophosphate	$<2.78 \times 10^{-5}$	6.85	1.8
3.84_312.9758	3.84	312.9758	HMDB06329	D-glucuronic acid 1-phosphate	$<7.54 \times 10^{-6}$	0.29	1.8
6.20_626.3522	6.20	626.3522	HMDB02579	Glycochenodeoxycholic acid 3-glucuronide	$<1.08 \times 10^{-5}$	3.30	1.6
6.66_607.3490	6.66	607.3490	HMDB06353	Dolichol phosphate	$<1.26 \times 10^{-5}$	0.40	1.3

VIP = variable importance in projection.

* Standard deviation step down-adjusted P value.

[†] Fold change (FC) was calculated from the ratio of the arithmetic mean values of peak intensity in each group. FC with a value >1.00 indicated that the concentration of certain metabolite was up-regulated in the relative group, while FC with a value <1.00 indicated that the concentration of certain metabolite was down-regulated in the relative group.

Table 2**Significantly changed metabolites involved in glucose metabolism (T3 vs T2).**

Primary ID	Retention time, min	Mass	HMDB ID	Metabolite name	<i>P</i> [*]	FC [†]	VIP
3.90_242.0815	3.90	242.0815	HMDB00201	L-acetylcarnitine	$<1.54 \times 10^{-5}$	0.61	1.9
6.37_507.1879	6.37	507.1879	HMDB06790	Galactosylglycerol	$<6.43 \times 10^{-5}$	0.17	1.8
8.92_485.2155	8.92	485.2155	HMDB10337	6-Dehydrotestosterone glucuronide	$<3.41 \times 10^{-6}$	1.47	1.6
6.04_579.2367	6.04	579.2367	HMDB00052	Argininosuccinic acid	$<3.42 \times 10^{-4}$	0.24	1.5
6.02_299.1148	6.02	299.1148	HMDB10350	2-Phenylethanol glucuronide	$<7.84 \times 10^{-6}$	0.48	1.5
0.65_144.0309	0.65	144.0309	HMDB01552	2-Keto-glutaramic acid	$<5.60 \times 10^{-6}$	1.63	1.4
6.21_626.3530	6.21	626.3530	HMDB02579	Glycochenodeoxycholic acid 3-glucuronide	$<1.49 \times 10^{-5}$	3.50	1.3
1.09_189.0044	1.09	189.0044	HMDB03974	Oxalosuccinic acid	$<1.19 \times 10^{-5}$	0.53	1.3

VIP = variable importance in projection.

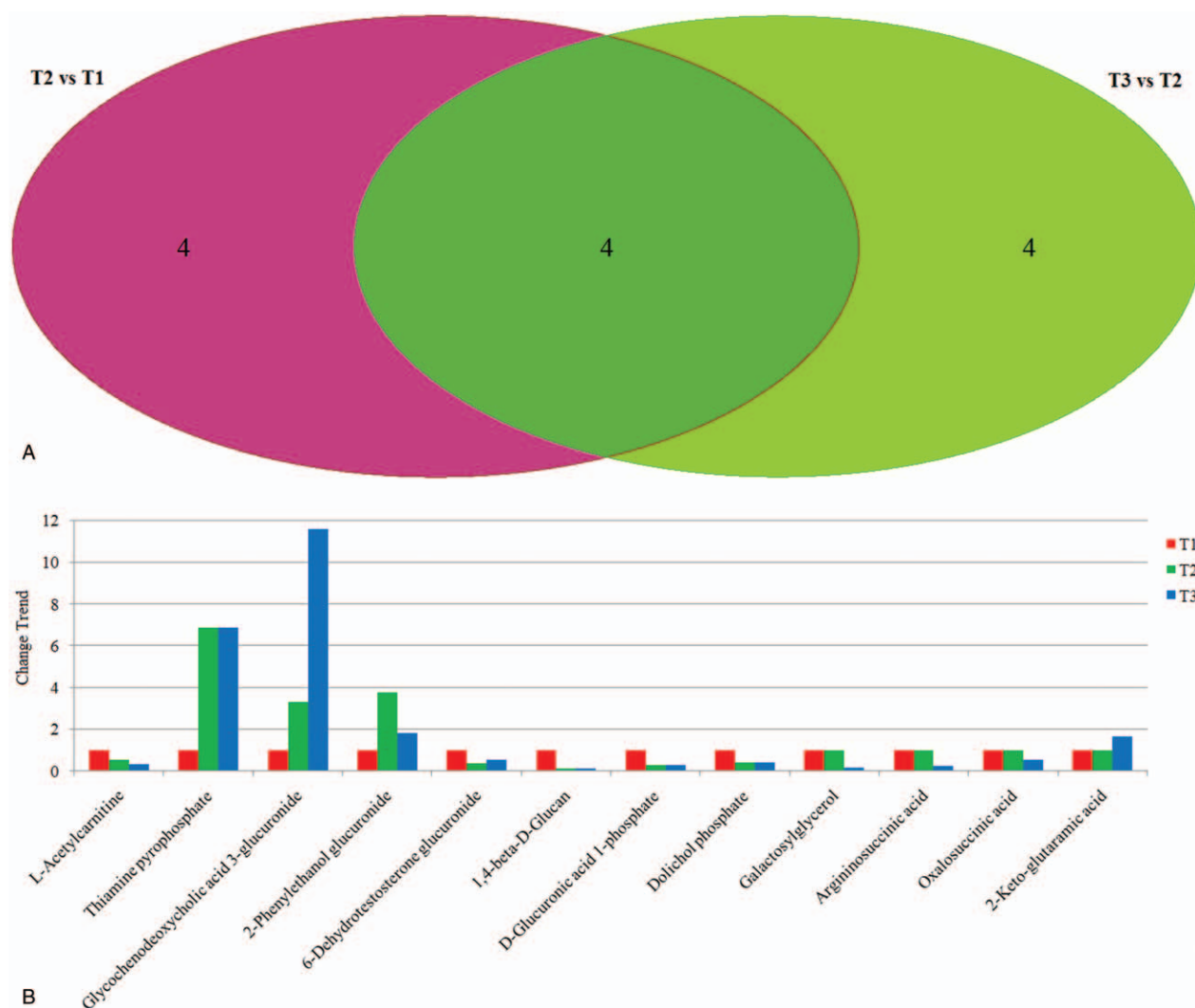
^{*}Standard deviation step down-adjusted *P* value.[†]Fold change (FC) was calculated from the ratio of the arithmetic mean values of each group. FC with a value >1.00 indicated that the concentration of certain metabolite was up-regulated in the relative group, while FC with a value <1.00 indicated that the concentration of certain metabolite was down-regulated in the relative group.

Figure 3. Metabolite change trends and overlap for significantly changed metabolites in different trimesters. (A) Venn diagram of the overlap of significantly changed metabolites involved in glucose metabolism in different trimesters. Four overlapped metabolites and 4 exclusive metabolites were screened out for T2 versus T1 and T3 versus T2, respectively. The overlapped metabolites were L-acetylcarnitine, 2-phenylethanol glucuronide, 6-dehydrotestosterone glucuronide, and glycochenodeoxycholic acid 3-glucuronide. The exclusive metabolites for T2 versus T1 were 1,4-beta-D-glucan, thiamine pyrophosphate, D-glucuronic acid 1-phosphate, and dolichol phosphate. The exclusive metabolites for T3 versus T2 were galactosylglycerol, argininosuccinic acid, 2-keto-glutaramic acid, and oxalosuccinic acid. (B) Relative dynamic trend of significantly changed metabolites. T1, T2, and T3 denote the first trimester, the second trimester, and the third trimester, respectively.

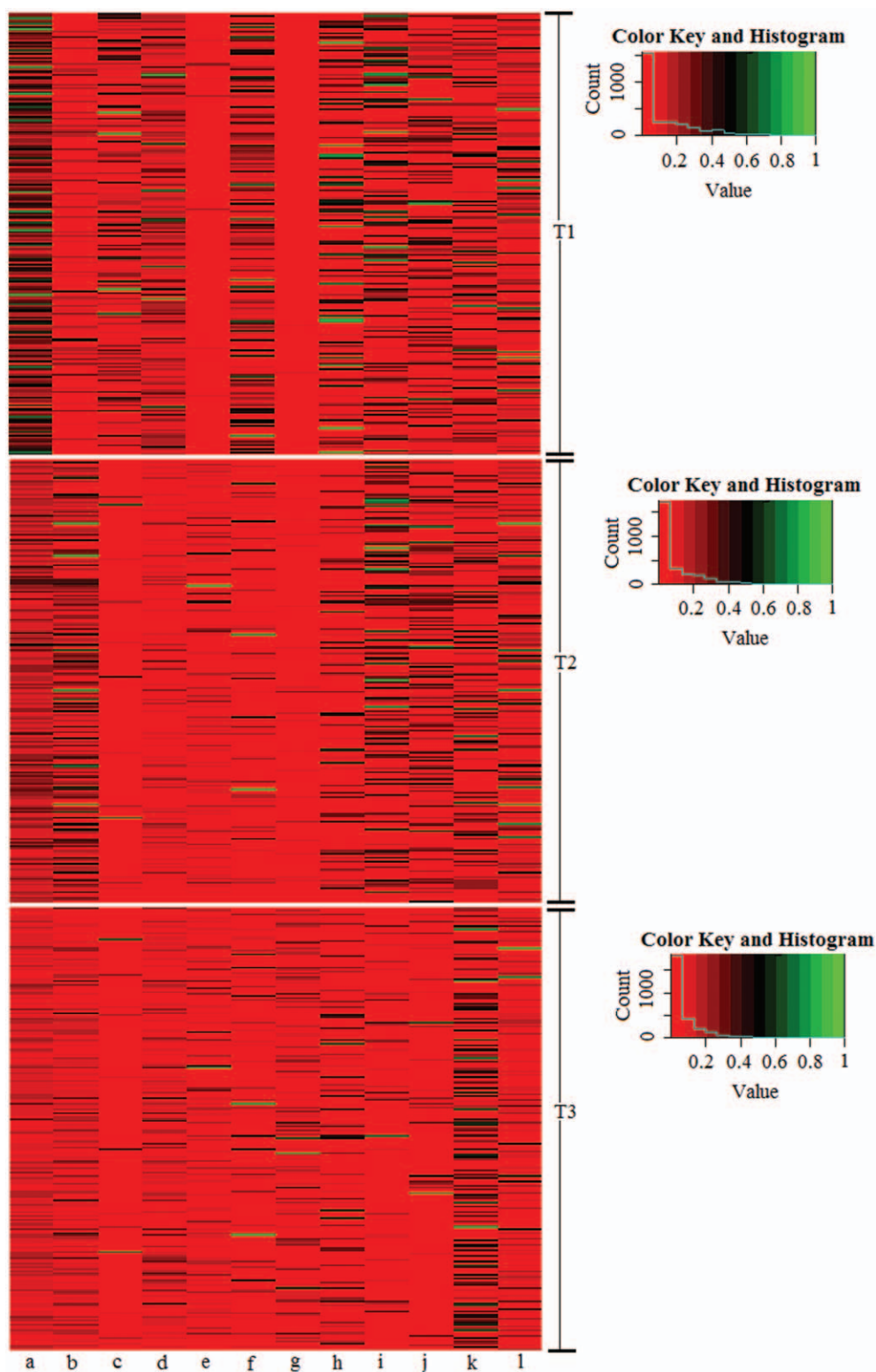


Figure 4. Heat map of the relative concentration of significantly changed metabolites involved in glucose metabolism in different trimesters. T1, T2, and T3 denote the first trimester, the second trimester, and the third trimester, respectively. (a) l-Acetylcarnitine; (b) 2-phenylethanol glucuronide; (c) 1,4-beta-D-glucan; (d) 6-dehydrotestosterone glucuronide; (e) thiamine pyrophosphate; (f) D-glucuronic acid 1-phosphate; (g) glycochenodeoxycholic acid 3-glucuronide; (h) dolichol phosphate; (i) galactosylglycerol; (j) argininosuccinic acid; (k) 2-keto-glutaramic acid; (l) oxalosuccinic acid.

stress during normal pregnancy.^[3,6] An important advantage of urine metabolites is that they represent the final state of metabolism, while the metabolites in the blood most likely continue to participate in metabolism. The urine metabolomics

approach of the present study, combined with the relatively large longitudinal cohort design, the more sensitive analytical platform, and the keen focus on the terminal products of glucose metabolism, may provide a critical characterization of glucose

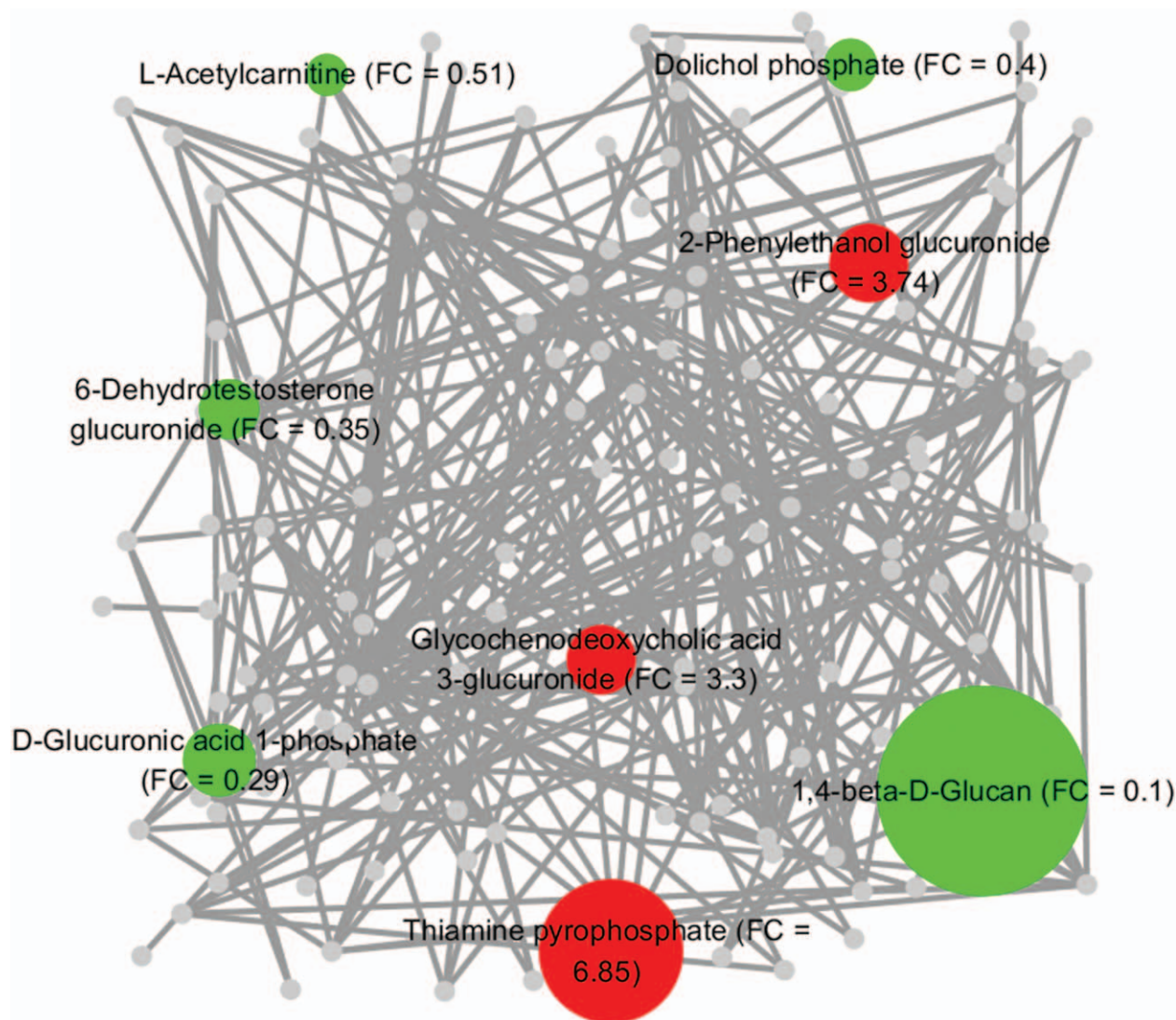


Figure 5. Glucose metabolic network generated from the significantly changed metabolites in the second trimester (compared with the first trimester). The chemical similarity and KEGG biochemical interpretation of the intermediates involved in glucose metabolism were integrated into the network visualization in Cytoscape using MetaMapp software. The red nodes denote the significantly elevated metabolites involved in glucose metabolism, the green nodes denote the significantly reduced metabolites involved in glucose metabolism, and the gray nodes denote the metabolites which were significantly changed in this study but not involved in glucose metabolism. The size of the colored nodes is coded by the corresponding fold change (FC) value. The network edges among the metabolites are defined by the thresholds of similarity scores (Tanimoto coefficients > 0.5). The nodes clustered closely have similar chemical structures and biochemical reaction modules.

metabolic stress during the progression of gestation. In this study, the urine metabolites that were most altered, along with their related metabolic pathways, were investigated in a longitudinal cohort of healthy women.

Glucose metabolism varies due to a significant difference in the level of maternal insulin sensitivity,^[27,28] and progressive insulin resistance is considered an underlying driver for many of the observed metabolic adaptations during normal pregnancy.^[10] L-acetylcarnitine is important in facilitating the movement of acetyl-CoA into the mitochondrial matrix to allow long-chain fatty acid oxidation, maintain energetic balance, and provide unique neuroprotective, neuromodulatory, and neurotrophic properties.^[29] Previous studies showed that L-acetylcarnitine was beneficial by downregulating the level of insulin resistance in insulin-resistant conditions, including obesity,^[30] diabetes,^[31] and human immunodeficiency virus.^[32] The relative concentra-

tion of L-acetylcarnitine was found to decline progressively during pregnancy (fold change [FC]=0.51, T2 vs T1; FC=0.61, T3 vs T2), which may be related to the decline in insulin sensitivity during the course of normal pregnancy.

Glucuronidation, which is catalyzed by UDP glucuronyltransferase, a mammalian superfamily of phase II metabolizing enzymes expressed in a variety of organs and tissues, including the human liver and placenta,^[33,34] contributes to the renal excretion of poisonous materials, drugs, or other substances by increasing their water solubility. In this study, 4 glucuronides (D-glucuronic acid 1-phosphate, 6-dehydrotestosterone glucuronide, 2-phenylethanol glucuronide, and GCDC 3-glucuronide) were screened out in the second trimester, and 3 (6-dehydrotestosterone glucuronide, 2-phenylethanol glucuronide, and GCDC 3-glucuronide) were screened out in the third trimester, as the metabolites most altered during the course of normal pregnancy.

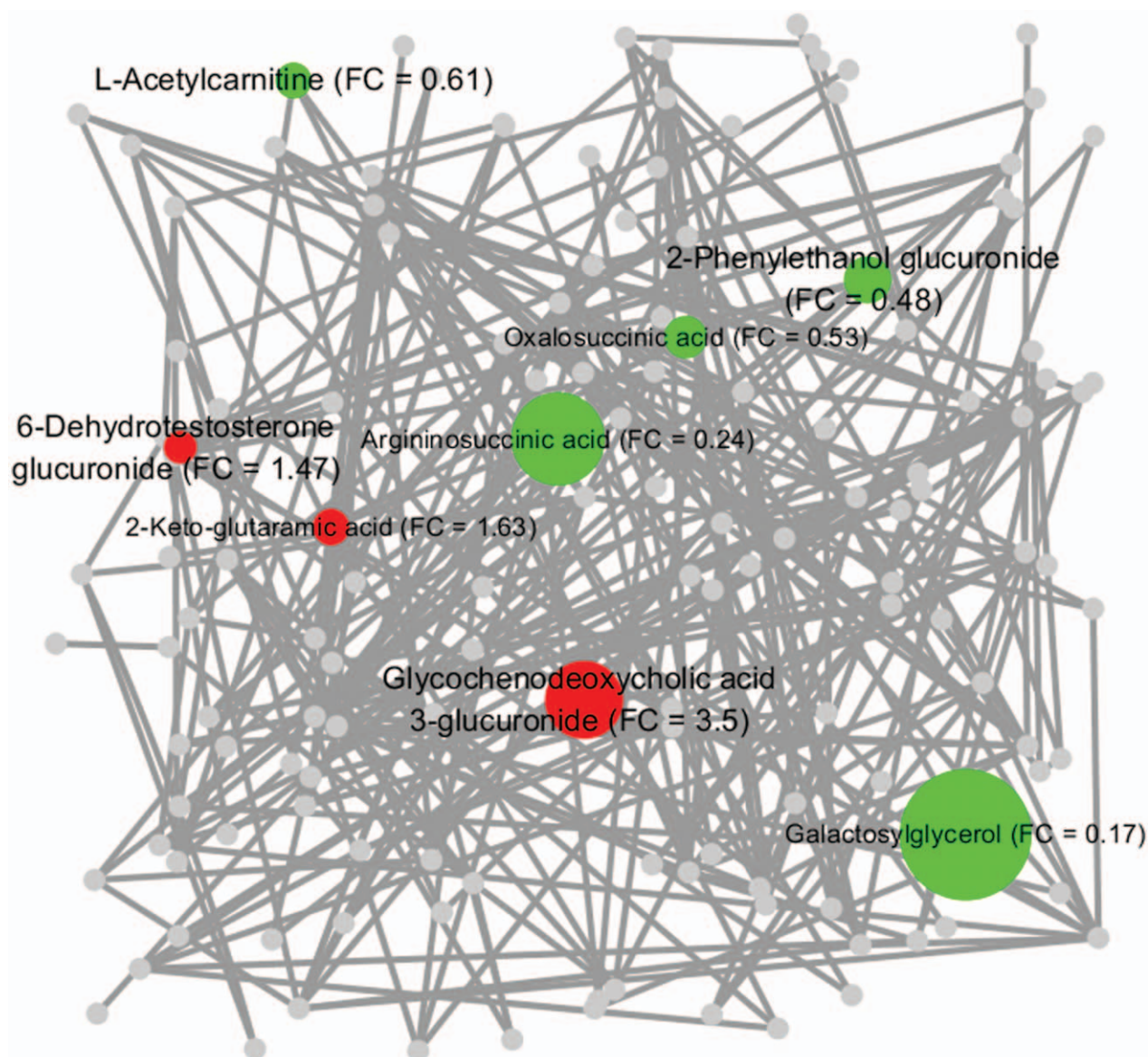


Figure 6. Glucose metabolic network generated from the significantly changed metabolites in the third trimester (compared with the second trimester). The chemical similarity and KEGG biochemical interpretation of the intermediates involved in glucose metabolism were integrated into the network visualization in Cytoscape using the MetaMapp software. The red nodes denote the significantly elevated metabolites involved in glucose metabolism, the green nodes denote the significantly reduced metabolites involved in glucose metabolism, and the gray nodes denote the metabolites which were significantly changed in this study but not involved in glucose metabolism. The size of the colored nodes is coded by the corresponding fold change (FC) value. The network edges among the metabolites are defined by the thresholds of similarity scores (Tanimoto coefficients > 0.5). The nodes clustered closely have similar chemical structures and biochemical reaction modules.

This finding indicated a substantial alteration in the metabolic pathway between UDP-D-glucuronate and D-glucuronate. Interestingly, 2-phenylethanol glucuronide, a waste product that is excreted by the kidney and is related to type 2 diabetes,^[35] was also screened out in the present longitudinal healthy pregnant cohort. Its concentration significantly increased in the second trimester (FC=3.74, T2 vs T1) but significantly decreased in the third trimester (FC=0.48, T3 vs T2), a pattern that may improve our understanding of pregnancy-induced abnormal glucose metabolism and may provide a valuable clue for further studies. GCDC, a metabolite of bile acids, was believed to cause hepatocellular necrosis and apoptosis in part by inducing the mitochondrial permeability transition and the mitochondrial generation of oxidative radicals.^[36] In this study, the concentra-

tion of GCDC 3-glucuronide, a glucuronide of GCDC, progressively increased as pregnancy progressed (FC=3.3, T2 vs T1; FC=3.5, T3 vs T2), which may be explained by the adaptive protection of the maternal body from liver injury by increasing the excretion of GCDC.

Before the 3rd month of pregnancy, the level of fasting plasma glucose remains constant in the maternal body. Thereafter, the plasma glucose level decreases by 10 to 15 mg/dL as the plasma insulin concentration increases twofold.^[1] Under this condition, the endogenous production of glucose is almost completely accounted for by gluconeogenesis and is enhanced by 16% to 30%.^[1,28] In this study, the concentration of thiamine pyrophosphate, an intermediate involved in glycolysis/gluconeogenesis, was found to be increased 6.85-

fold (FC = 6.85, T2 vs T1) in the second trimester. Furthermore, the concentration of 2-keto-glutamic acid, an intermediate involved in glycolytic amino acid (alanine) metabolism, was increased 1.63-fold (FC = 1.63, T3 vs T2) in the third trimester; this increase may be due to the normal pregnancy-induced enhancement of gluconeogenesis.

The concentrations of both oxalosuccinic acid, an intermediate in the TCA cycle, and argininosuccinic acid, a precursor of fumaric acid, were decreased in the third trimester, suggesting a possible reduction in demand for the TCA cycle, a change that probably results because the aerobic oxidation of glucose is reduced to ensure an adequate glucose supply for fetal development during late pregnancy. The concentration of galactosylglycerol, an intermediate involved in galactose metabolism, did not change remarkably in the second trimester but significantly decreased in the third trimester, a pattern that can be explained by the rapidly increased demand for this metabolite during fetal development. 1,4-Beta-D-glucan, a polymer of glucose molecules involved in nonabsorbable carbohydrate metabolism, was detected in this study and its concentration showed a trend of significant decrease in the second trimester (FC = 0.1, T2 vs T1), indicating a significant decrease in cellulose and other nonabsorbable carbohydrates as pregnancy progressed. However, further evidence is needed to validate this hypothesis.

The UPLC-QTOFMS-based untargeted metabolomics analysis also revealed pregnancy-induced changes in N-glycosylation, which is one of the most important means of the posttranslational modification of proteins and has complex biological functions in processes including tumorigenesis,^[37] the immune response,^[38,39] and cell communication.^[40] Pregnancy-related N-glycosylation has been examined in a few studies.^[41–45] In this study, the concentration of dolichol phosphate, an intermediate involved in N-glycan biosynthesis, decreased significantly in the second trimester and was maintained at a low level in the third trimester, which may indicate that normal pregnancy induced a considerable inhibition of N-glycosylation.

This study has some limitations. First, the results from this study are only applicable to pregnant women, limiting the results from being applied to the entire female population. In a future study, we will include a cohort of control subjects to acquire more data about the differences between the nonpregnant cohort and the pregnant cohort. Second, the content of the metabolites was not quantified absolutely, but the relative quantification accurately reflects the trends of the changes in the metabolites. Third, the changes in the physiological parameters of the kidney were not fully taken into account in the analysis of the alteration of urine metabolites during pregnancy.

5. Conclusion

This work employed a UPLC-QTOFMS approach to determine the dynamic changes in glucose metabolism-associated intermediates among a large cohort of healthy women in different trimesters of pregnancy. Twelve metabolites related to glucose metabolism were identified, and their variations throughout pregnancy were followed, thus providing a relatively detailed dynamic signature of glucose metabolism during normal pregnancy. Within the discovered variations, metabolites in the metabolic networks of insulin resistance, pentose and glucuronate interconversion, glycolysis/gluconeogenesis, TCA cycle, nonabsorbable carbohydrate metabolism, and N-glycan biosynthesis were comprehensively observed in connection with normal pregnancy. This normal pregnancy-related glucose metabolic

profile as well as the pathway information might help in the exploration of the complex mechanisms underlying physiological metabolic stress and might have the potential to allow the generation of a novel hypothesis about glucose metabolism. In turn, such a hypothesis could provide an ideal base for a large-scale epidemiological study of women who subsequently develop pregnancy-related metabolic abnormalities, for example, gestational diabetes.

Author contributions

Conceptualization: Shunqing Xu, Songfeng Lu.

Data curation: Wei Xia, Han Li.

Formal analysis: Mu Wang.

Funding acquisition: Shunqing Xu.

Investigation: Mu Wang, Han Li.

Methodology: Xiaojie Sun.

Supervision: Shunqing Xu.

Writing – original draft: Mu Wang.

Writing – review & editing: Mu Wang, Wei Xia, Fang Liu, Yuanyuan Li, Songfeng Lu, Shunqing Xu.

References

- [1] Di Cianni G, Miccoli R, Volpe L, et al. Intermediate metabolism in normal pregnancy and in gestational diabetes. *Diabetes Metab Res Rev* 2003;19:259–70.
- [2] Drynda R, Peters CJ, Jones PM, Bowe JE. The role of non-placental signals in the adaptation of islets to pregnancy. *Horm Metab Res* 2015;47:64–71.
- [3] Angueira AR, Ludvik AE, Reddy TE, et al. New insights into gestational glucose metabolism: lessons learned from 21st century approaches. *Diabetes* 2015;64:327–34.
- [4] Horgan RP, Clancy OH, Myers JE, Baker PN. An overview of proteomic and metabolomic technologies and their application to pregnancy research. *BJOG* 2009;116:173–81.
- [5] Fanos V, Atzori L, Makarenko K, et al. Metabolomics application in maternal-fetal medicine. *Biomed Res Int* 2013;2013:720514.
- [6] Wang M, Liang Q, Li H, et al. Normal pregnancy-induced amino acid metabolic stress in a longitudinal cohort of pregnant women: novel insights generated from UPLC-QTOFMS-based urine metabolomic study. *Metabolomics* 2016;12:1–1.
- [7] Diaz SO, Barros AS, Goodfellow BJ, et al. Following healthy pregnancy by nuclear magnetic resonance (NMR) metabolic profiling of human urine. *J Proteome Res* 2013;12:969–79.
- [8] Luan H, Meng N, Liu P, et al. Pregnancy-induced metabolic phenotype variations in maternal plasma. *J Proteome Res* 2014;13:1527–36.
- [9] Pinto J, Barros AS, Domingues MR, et al. Following healthy pregnancy by NMR metabolomics of plasma and correlation to urine. *J Proteome Res* 2015;14:1263–74.
- [10] Lindsay KL, Hellmuth C, Uhl O, et al. Longitudinal metabolomic profiling of amino acids and lipids across healthy pregnancy. *PLoS ONE* 2015;10:e0145794.
- [11] Cho YM, Kim TH, Lim S, et al. Type 2 diabetes-associated genetic variants discovered in the recent genome-wide association studies are related to gestational diabetes mellitus in the Korean population. *Diabetologia* 2009;52:253–61.
- [12] Kwak SH, Kim SH, Cho YM, et al. A genome-wide association study of gestational diabetes mellitus in Korean women. *Diabetes* 2012;61:531–41.
- [13] Robitaille J, Grant AM. The genetics of gestational diabetes mellitus: evidence for relationship with type 2 diabetes mellitus. *Genet Med* 2008;10:240–50.
- [14] Freathy RM, Hayes MG, Urbanek M, et al. Hyperglycemia and Adverse Pregnancy Outcome (HAPO) study: common genetic variants in GCK and TCF7L2 are associated with fasting and postchallenge glucose levels in pregnancy and with the new consensus definition of gestational diabetes mellitus from the International Association of Diabetes and Pregnancy Study Groups. *Diabetes* 2010;59:2682–9.
- [15] Zhang C, Bao W, Rong Y, et al. Genetic variants and the risk of gestational diabetes mellitus: a systematic review. *Hum Reprod Update* 2013;19:376–90.

- [16] Lenz EM, Bright J, Wilson ID, et al. A ¹H NMR-based metabolomic study of urine and plasma samples obtained from healthy human subjects. *J Pharm Biomed Anal* 2003;33:1103–15.
- [17] Newgard CB, An J, Bain JR, et al. A branched-chain amino acid-related metabolic signature that differentiates obese and lean humans and contributes to insulin resistance. *Cell Metab* 2009;9:311–26.
- [18] Menni C, Fauman E, Erte I, et al. Biomarkers for type 2 diabetes and impaired fasting glucose using a nontargeted metabolomics approach. *Diabetes* 2013;62:4270–6.
- [19] Newgard CB. Interplay between lipids and branched-chain amino acids in development of insulin resistance. *Cell Metab* 2012;15:606–14.
- [20] Wang B, Shi Z, Weber GF, Kennedy MA. Introduction of a new critical p value correction method for statistical significance analysis of metabolomics data. *Anal Bioanal Chem* 2013;405:8419–29.
- [21] Want EJ, Wilson ID, Gika H, et al. Global metabolic profiling procedures for urine using UPLC-MS. *Nat Protoc* 2010;5:1005–18.
- [22] Goodpaster AM, Romick-Rosendale LE, Kennedy MA. Statistical significance analysis of nuclear magnetic resonance-based metabolomics data. *Anal Biochem* 2010;401:134–43.
- [23] Liang Q, Xu W, Hong Q, et al. Rapid comparison of metabolites in humans and rats of different sexes using untargeted UPLC-TOFMS and an in-house software platform. *Eur J Mass Spectrom (Chichester, Eng)* 2015;21:801–21.
- [24] Shannon P, Markiel A, Ozier O, et al. Cytoscape: a software environment for integrated models of biomolecular interaction networks. *Genome Res* 2003;13:2498–504.
- [25] Barupal DK, Haladiya PK, Wohlgemuth G, et al. MetaMapp: mapping and visualizing metabolomic data by integrating information from biochemical pathways and chemical and mass spectral similarity. *BMC Bioinformatics* 2012;13:99.
- [26] Meissen JK, Yuen BT, Kind T, et al. Induced pluripotent stem cells show metabolomic differences to embryonic stem cells in polyunsaturated phosphatidylcholines and primary metabolism. *PLoS ONE* 2012;7:e46770.
- [27] Lain KY, Catalano PM. Metabolic changes in pregnancy. *Clin Obstet Gynecol* 2007;50:938–48.
- [28] Butte NF. Carbohydrate and lipid metabolism in pregnancy: normal compared with gestational diabetes mellitus. *Am J Clin Nutr* 2000;71(suppl):1256S–61S.
- [29] Virmani A, Binienda Z. Role of carnitine esters in brain neuropathology. *Mol Aspects Med* 2004;25:533–49.
- [30] Wutzke KD, Lorenz H. The effect of L-carnitine on fat oxidation, protein turnover, and body composition in slightly overweight subjects. *Metabolism* 2004;53:1002–6.
- [31] Mingrone G, Greco AV, Capristo E, et al. L-carnitine improves glucose disposal in type 2 diabetic patients. *J Am Coll Nutr* 1999;18:77–82.
- [32] Benedini S, Perseghin G, Terruzzi I, et al. Effect of L-acetylcarnitine on body composition in HIV-related lipodystrophy. *Horm Metab Res* 2009;41:840–5.
- [33] Reimers A, Østby L, Stuen I, Sundby E. Expression of UDP-glucuronosyltransferase 1A4 in human placenta at term. *Eur J Drug Metab Pharmacokinet* 2011;35:79–82.
- [34] Pacifici GM, Rane A. Distribution of UDP-glucuronyltransferase in different human foetal tissues. *Br J Clin Pharmacol* 1982;13:732–5.
- [35] Sun H, Zhang S, Zhang A, et al. Metabolomic analysis of diet-induced type 2 diabetes using UPLC/MS integrated with pattern recognition approach. *PLoS ONE* 2014;9:e93384.
- [36] Sokol RJ, Dahl R, Devereaux MW, et al. Human hepatic mitochondria generate reactive oxygen species and undergo the permeability transition in response to hydrophobic bile acids. *J Pediatr Gastroenterol Nutr* 2005;41:235–43.
- [37] Dube DH, Bertozzi CR. Glycans in cancer and inflammation—potential for therapeutics and diagnostics. *Nat Rev Drug Discov* 2005;4:477–88.
- [38] Hayes JM, Frostell A, Cosgrave EF, et al. Fc gamma receptor glycosylation modulates the binding of IgG glycoforms: a requirement for stable antibody interactions. *J Proteome Res* 2014;13:5471–85.
- [39] Freire T, Osinaga E. The sweet side of tumor immunotherapy. *Immunotherapy* 2012;4:719–34.
- [40] Pinho SS, Reis CA. Glycosylation in cancer: mechanisms and clinical implications. *Nat Rev Cancer* 2015;15:540–55.
- [41] Robajac D, Masnikosa R, Vanhooren V, et al. The N-glycan profile of placental membrane glycoproteins alters during gestation and aging. *Mech Ageing Dev* 2014;138:1–9.
- [42] Valmu L, Alftan H, Hotakainen K, et al. Site-specific glycan analysis of human chorionic gonadotropin beta-subunit from malignancies and pregnancy by liquid chromatography–electrospray mass spectrometry. *Glycobiology* 2006;16:1207–18.
- [43] Orczyk-Pawilowicz M, Hirnle L, Katnik-Prastowska I. Alterations of N-glycan branching and expression of sialic acid on amniotic fluid alpha-1-acid glycoprotein derived from second and third trimesters of normal and prolonged pregnancies. *Clin Chim Acta* 2006;367:86–92.
- [44] Jeschke U, Gundel G, Müller H, et al. N-glycans of human amniotic fluid transferrin stimulate progesterone production in human first trimester trophoblast cells in vitro. *J Perinat Med* 2004;32:248–53.
- [45] Jones CJ, Jauniaux E, Stoddart RW. Glycans of the early human yolk sac. *Histochem J* 1995;27:210–21.